Frontiers in Heat and Mass Transfer

Tech Science Press

Doi:10.32604/fhmt.2025.063023

ARTICLE

Heat Transfer and Flow Dynamics of Ternary Hybrid Nanofluid over a Permeable Disk under Magnetic Field and Joule Heating Effects

Umi Nadrah Hussein[1], **Najiyah Safwa Khashi'ie**[1,*], **Norihan Md Arifin**[2] **and Ioan Pop**[3]

[1]Fakulti Teknologi dan Kejuruteraan Mekanikal, Universiti Teknikal Malaysia Melaka, Hang Tuah Jaya, Durian Tunggal, Melaka, 76100, Malaysia
[2]Department of Mathematics and Statistics, Faculty of Science, Universiti Putra Malaysia, Serdang, 43400, Malaysia
[3]Department of Mathematics, Babeş-Bolyai University, Cluj-Napoca, 400084, Romania

*Corresponding Author: Najiyah Safwa Khashi'ie. Email: najiyah@utem.edu.my

Received: 02 January 2025; Accepted: 27 February 2025; Published: 25 April 2025

ABSTRACT: This study investigates the heat transfer and flow dynamics of a ternary hybrid nanofluid comprising alumina, copper, and silica/titania nanoparticles dispersed in water. The analysis considers the effects of suction, magnetic field, and Joule heating over a permeable shrinking disk. A mathematical model is developed and converted to a system of differential equations using similarity transformation which then, solved numerically using the bvp4c solver in Matlab software. The study introduces a novel comparative analysis of alumina-copper-silica and alumina-copper-titania nanofluids, revealing distinct thermal conductivity behaviors and identifying critical suction values necessary for flow stabilization. Dual solutions are found within a specific range of parameters such that the minimum required suction values for flow stability, with $S_c = 1.2457$ for alumina-copper-silica/water and $S_c = 1.2351$ for alumina-copper-titania/water. The results indicate that increasing suction by 1% enhances the skin friction coefficient by up to 4.17% and improves heat transfer efficiency by approximately 1%, highlighting its crucial role in stabilizing the opposing flow induced by the shrinking disk. Additionally, the inclusion of 1% silica nanoparticles reduces both skin friction and heat transfer rate by approximately 0.28% and 0.85%, respectively, while 1% titania concentration increases skin friction by 3.02% but results in a slight heat transfer loss of up to 0.61%. These findings confirm the superior thermal performance of alumina-copper-titania/water, making it a promising candidate for enhanced cooling systems, energy-efficient heat exchangers, and industrial thermal management applications.

KEYWORDS: Dual solutions; Joule heating; magnetic field; shrinking disk; suction; ternary hybrid nanofluid

1 Introduction

Nanofluids, with their ability to significantly enhance heat transfer efficiency and optimize energy consumption, have emerged as a transformative innovation in engineerinssg processes, revolutionizing applications in energy systems, thermal management, and advanced manufacturing technologies [1–3]. Among them, hybrid nanofluid, formed by blending two or more types of nanoparticles in a base fluid, represents a groundbreaking advancement. By carefully selecting nanoparticle combinations, these fluids exhibit superior thermophysical properties as compared to traditional single-nanoparticle nanofluids, making them ideal for energy efficiency. Their exceptional thermal and physical characteristics have spurred extensive research into their applications, benefits, and limitations in diverse fields (see Nabil et al. [4], Adun et al. [5], Oladapo et al. [6], and Yu et al. [7]). Extensive research has been conducted on the boundary layer flow (BLF) of hybrid nanofluids, with early numerical investigations led by Takabi and Salehi [8] and Devi

Copyright © 2025 The Authors. Published by Tech Science Press.
This work is licensed under a Creative Commons Attribution 4.0 International License, which permits unrestricted use, distribution, and reproduction in any medium, provided the original work is properly cited.

and Devi [9], who examined the impact of hybrid nanoparticle suspensions on heat transfer enhancement over stretching surfaces. In addition, Devi et al. [10,11] also demonstrated the increased thermal conductivity and flow stability of hybrid nanofluids over traditional nanofluids. Since then, many researchers opted the thermophysical properties of the hybrid nanofluid as highlighted by Takabi et al. [8] and Devi et al. [9] in the studies of boundary layer flow subjected to various surfaces. As research progressed, Waqas et al. [12], Khan et al. [13], Bilal et al. [14], Khashi'ie et al. [15,16], Li et al. [17], Ali et al. [18] and Tassaddiq et al. [19] explored hybrid nanofluid dynamics over permeable and radially shrinking/stretching surfaces, revealing the influence of magnetohydrodynamics (MHD), velocity slip, and thermal radiation on heat and mass transfer. Meanwhile, Rahman et al. [20] focused on MHD-driven hybrid nanofluid flow over a rotating disk, highlighting the occurrence of dual solutions, boundary layer separation, and the role of heat generation in modifying energy transfer mechanisms. However, despite these advances, several critical gaps remain in the understanding of hybrid nanofluid behaviour, particularly in ternary hybrid nanofluids, which incorporate three distinct nanoparticles to achieve even greater control over thermophysical properties.

Expanding on this concept, ternary hybrid nanofluid (THNF), which integrates three distinct nanoparticles, provides further advancements by offering greater control over properties such as thermal conductivity, viscosity, and stability. Recent numerical studies have investigated the behaviour of these fluids under complex physical conditions, including magnetic fields, velocity and thermal slip, radiation, heat generation or absorption, and suction effects. For example, Jamrus et al. [21] demonstrated enhanced heat transfer performance with the increase of titania concentration in a copper-alumina-titania/water nanofluid model. Furthermore, dual solutions for ternary hybrid nanofluid Hiemenz flow over a shrinking surface have been analyzed by Jamrus et al. [22], who found that ternary hybrid, such as Cu-Al_2O_3-TiO_2, achieved higher skin friction and heat transfer coefficients as compared to hybrid nanofluid like Cu-Al_2O_3. Hussein et al. [23,24] numerically studied the ternary nanofluid flow induced by a shrinking cylinder with velocity slip and Joule heating effects, respectively. Mahmood et al. [25,26] analyzed THNF flow over a curved surface with suction and Lorentz force, focusing on momentum and thermal boundary layer modifications. However, they did not evaluate minimum suction requirements for flow stability, which is a significant component of this study. Mumtaz et al. [27,28] and Shinwari et al. [29] conducted a series of studies on radiative THNF flow in porous media and curved geometries, incorporating multiple slip constraints and cross-diffusion effects. While their models advanced the understanding of THNF behaviour in complex environments, they did not address the stability implications of dual solutions in suction-induced shrinking flows. Alharbi [30] investigated slip flow of THNF with suction, showing that heat transport is strongly influenced by suction variations. However, the study did not focus on comparative thermal performance between different ternary nanoparticle compositions, a key contribution of the present work.

The study of MHD (magnetohydrodynamic) flows in nanofluids has been extensively conducted, particularly in the context of fractional order derivatives and modified heat transfer models. For example, Khan et al. [31] applied advanced numerical simulations using distributed fractional-order derivatives and the Cattaneo heat flux model to analyze MHD fluid flow, demonstrating the importance of non-Fourier heat conduction in energy transport. However, these approaches have yet to be systematically applied to ternary hybrid nanofluids subjected to suction and Joule heating, which is a key focus of this study. Furthermore, artificial intelligence-driven models, such as artificial neural networks (ANNs), have been employed to predict heat and mass transfer behaviour in chemically reactive fluids over complex surfaces. While Khan et al. [32] used ANN-based techniques to analyze heat transfer dynamics across variable-thickness surfaces, this study focuses on solving nonlinear coupled differential equations using the bvp4c solver. These data-driven methodologies offer potential future extensions for optimizing THNF-based cooling systems in energy-efficient industrial processes.

Despite significant progress in the study of nanofluids, there remains a limited understanding of ternary hybrid nanofluids under the combined influences of suction, Joule heating, and disk surface. To address this limitation, the current study delves into the flow and thermal characteristics of a ternary hybrid nanofluid, specifically copper-alumina-titania/water, over a shrinking disk. The investigation incorporates crucial parameters, including suction, Joule heating, and magnetic field effects, to emulate realistic conditions encountered in engineering systems. Suction is particularly emphasized due to its role in stabilizing reverse flow originating from shrinking surfaces. Many researchers have highlighted the importance of suction in maintaining the reverse flow due to shrinking surface (see Jamrus et al. [33], Memon et al. [34]). By analyzing dual solutions, identifying critical separation points, and assessing the influence of physical parameters, this study seeks to advance the understanding of ternary hybrid nanofluids. A single-phase nanofluid model forms the basis of this numerical study, where governing partial differential equations (PDEs) are transformed into a system of ordinary differential equations (ODEs) via similarity transformation. The resulting equations are solved using the bvp4c solver. To validate the model's accuracy, numerical findings are compared with previously reported results under specific conditions. The insights gained from this research contribute to the enhancement of thermal management strategies and provide a foundation for future advancements in energy-efficient technologies.

This study extends existing research by analyzing the behaviour of ternary hybrid nanofluids (alumina-copper-silica and alumina-copper-titania) under these external influences over a permeable shrinking disk. The novelty of this work lies in the following:

- Comparative analysis of two ternary hybrid nanofluids to evaluate differences in heat transfer efficiency and flow stability.
- Identification of critical suction values necessary to maintain flow stability, which is essential for optimizing fluid-based thermal management systems.
- Dual solution analysis, reveals non-unique flow behaviour, which is important for practical applications where multiple stable/unstable flow regimes can occur.

By addressing these aspects, this study advances the state of knowledge in nanofluid-based thermal management, providing valuable insights for optimizing energy systems, high-performance cooling devices, and industrial heat exchangers. The findings also establish a foundation for future research on complex nanofluid behaviour under dynamic operating conditions.

2 Problem Formulation

This study examines the symmetrical flow behavior of a THNF, composed of aluminum oxide (Al_2O_3), copper (Cu), and titanium dioxide (TiO_2) nanoparticles suspended in a water medium, interacting with a disk undergoing stretching or shrinking motion. The influence of both magnetic force and velocity slip is considered to evaluate their impact on the heat transfer characteristic. Using a cylindrical coordinate system (r, φ, z), the analysis assumes axial symmetry $(\partial/\partial\varphi = 0)$ and focuses on the region where $z \geq 0$. The velocity of the disk is mathematically represented as $u_w(r) = ar$, with a as a constant parameter. The temperature at the surface of the disk is in a variable form represented as $T_w = T_\infty + T_0 (r/L)^2$, where T_∞ is the ambient temperature, T_0 is the characteristic temperature and L is the characteristic length of the disk. In order to simplify the mathematical framework while maintaining the physical accuracy, the single-phase nanofluid model is employed. The primary assumptions are as follows:

- Nanoparticles are homogeneously dispersed in the base fluid, ensuring a uniform thermophysical response.
- No nanoparticle aggregation occurs, meaning that Brownian motion and thermophoresis are neglected.

- Thermal equilibrium is assumed between the nanoparticles and the base fluid, meaning that all nanoparticles and the surrounding fluid share the same temperature field. Several studies have validated the single-phase nanofluid model for moderate nanoparticle volume fractions ($\phi \leq 1\%$), showing that it provides accurate predictions without significantly deviating from more complex two-phase models. The foundational study by Buongiorno [35] showed that for low nanoparticle volume fractions ($\leq 1\%$), the effect of Brownian motion and thermophoresis is negligible, making the single-phase model a valid assumption.

This model is widely used in boundary layer nanofluid studies and has been validated in previous research, including Khashi'ie et al. [15] and Jamrus et al. [33]. The enhanced physical properties of the ternary nanofluid are embedded into the governing equations that describe flow and thermal transport. These mathematical formulations are constructed from conservation laws for momentum and energy and are customized for this specific nanofluid system, utilizing established methodologies from previous literature (see Khashi'ie et al. [15], Jamrus et al. [33]).

$$\frac{\partial}{\partial r}(ru) + \frac{\partial}{\partial z}(rv) = 0, \tag{1}$$

$$u\frac{\partial u}{\partial r} + v\frac{\partial u}{\partial z} = \frac{\mu_{thnf}}{\rho_{thnf}}\frac{\partial^2 u}{\partial z^2} - \frac{\sigma_{thnf}{B_0}^2 u}{\rho_{thnf}}, \tag{2}$$

$$u\frac{\partial T}{\partial r} + v\frac{\partial T}{\partial z} = \frac{k_{thnf}}{\left(\rho C_p\right)_{thnf}}\frac{\partial^2 T}{\partial z^2} + \frac{\sigma_{thnf}{B_0}^2 u^2}{\left(\rho C_p\right)_{thnf}}, \tag{3}$$

while the boundary conditions are:

$$\begin{aligned} &v = v_0, u = \lambda u_w(r), T = T_w(r) \text{ at } z = 0, \\ &u \to 0, T \to T_\infty \text{ as } z \to \infty. \end{aligned} \tag{4}$$

The velocity components in the radial (r) and axial (z) directions are denoted by u and v, respectively, while the temperature is indicated as T. Meanwhile, B_0 represents the constant magnetic field strength which directed perpendicular to the disk surface. The stretching/shrinking behaviour of the disk is governed by the parameter λ, where $\lambda > 0$ represents a stretching disk, $\lambda < 0$ corresponds to a shrinking disk, and $\lambda = 0$ describes a static disk. The mass flow condition at the boundary condition (4) is modeled as $v_0 = -2S\sqrt{av_f}$ (see Jamrus et al. [33]). Positive values of S signify suction, which is utilized throughout this study to stabilize the opposing flow. Table 1 outlines the correlations employed to calculate the thermophysical properties of the ternary hybrid nanofluid. The symbols ϕ_1, ϕ_2, ϕ_3 represent the volumetric concentrations of Al_2O_3, Cu, and TiO_2 nanoparticles, respectively. The subscripts *thnf*, *f*, s_1, s_2, s_3 refer to the ternary nanofluid, base fluid, and the individual Al_2O_3, Cu, and TiO_2 nanoparticles, respectively. Table 2 provides the material properties, including thermal conductivity, density, and specific heat, for both the base fluid and the nanoparticles utilized in this analysis.

In boundary layer flow analysis, similarity transformations are crucial in reducing the complexity of partial differential equations (PDEs) into ordinary differential equations (ODEs). The transformations chosen in this study are derived based on physical considerations of the problem and prior research on shrinking/stretching flows in nanofluids. Similarity transformations which fulfill Eq. (1) are based on previous literature on disk flow (see Khashi'ie et al. [15], Jamrus et al. [33]).

$$u = arf'(\eta), v = -2\sqrt{av_f}f(\eta), \theta(\eta) = \frac{T - T_\infty}{T_w - T_\infty}, \eta = z\sqrt{a/v_f}. \tag{5}$$

Table 1: Correlations of thermophysical properties for hybrid nanofluids

Properties	Ternary Nanofluid (THNF) & Hybrid Nanofluid (HNF)
Density	$\rho_{thnf} = (1-\phi_3)\left\{(1-\phi_2)\left[(1-\phi_1)\rho_f + \phi_1\rho_{s1}\right] + \phi_2\rho_{s2}\right\} + \phi_3\rho_{s3}$ $\rho_{hnf} = (1-\phi_2)\left[(1-\phi_1)\rho_f + \phi_1\rho_{s1}\right] + \phi_2\rho_{s2}$
Heat capacity	$\left(\rho C_p\right)_{thnf} = (1-\phi_3)\left\{(1-\phi_2)\left[(1-\phi_1)\left(\rho C_p\right)_f + \phi_1\left(\rho C_p\right)_{s1}\right] + \phi_2\left(\rho C_p\right)_{s2}\right\} + \phi_3\left(\rho C_p\right)_{s3}$ $\left(\rho C_p\right)_{hnf} = (1-\phi_2)\left[(1-\phi_1)\left(\rho C_p\right)_f + \phi_1\left(\rho C_p\right)_{s1}\right] + \phi_2\left(\rho C_p\right)_{s2}$
Dynamic viscocity	$\frac{\mu_{thnf}}{\mu_f} = \frac{1}{(1-\phi_1)^{2.5}(1-\phi_2)^{2.5}(1-\phi_3)^{2.5}}$ $\frac{\mu_{hnf}}{\mu_f} = \frac{1}{(1-\phi_1)^{2.5}(1-\phi_2)^{2.5}}$
Thermal conductivity	$\frac{k_{thnf}}{k_{hnf}} = \left[\frac{k_{s3}+2k_{hnf}-2\phi_3\left(k_{hnf}-k_{s3}\right)}{k_{s3}+2k_{hnf}+\phi_3\left(k_{hnf}-k_{s3}\right)}\right]$ where $\frac{k_{hnf}}{k_{nf}} = \left[\frac{k_{s2}+2k_{nf}-2\phi_2\left(k_{nf}-k_{s2}\right)}{k_{s2}+2k_{nf}+\phi_2\left(k_{nf}-k_{s2}\right)}\right]$ $\frac{k_{nf}}{k_f} = \left[\frac{k_{s1}+2k_f-2\phi_1\left(k_f-k_{s1}\right)}{k_{s1}+2k_f+\phi_1\left(k_f-k_{s1}\right)}\right]$
Electrical conductivity	$\frac{\sigma_{thnf}}{\sigma_{hnf}} = \left[\frac{\sigma_{s3}+2\sigma_{hnf}-2\phi_3\left(\sigma_{hnf}-\sigma_{s3}\right)}{\sigma_{s3}+2\sigma_{hnf}+\phi_3\left(\sigma_{hnf}-\sigma_{s3}\right)}\right]$ where $\frac{\sigma_{hnf}}{\sigma_{nf}} = \left[\frac{\sigma_{s2}+2\sigma_{nf}-2\phi_2\left(\sigma_{nf}-\sigma_{s2}\right)}{\sigma_{s2}+2\sigma_{nf}+\phi_2\left(\sigma_{nf}-\sigma_{s2}\right)}\right]$ $\frac{\sigma_{nf}}{\sigma_f} = \left[\frac{\sigma_{s1}+2\sigma_f-2\phi_1\left(\sigma_f-\sigma_{s1}\right)}{\sigma_{s1}+2\sigma_f+\phi_1\left(\sigma_f-\sigma_{s1}\right)}\right]$

Table 2: Properties of nanoparticles and water

Physical properties	Cu	Al_2O_3	SiO_2	TiO_2	Water
$\rho\,(\mathrm{kg/m^3})$	8933	3970	4250	2200	997.1
$C_p\,(\mathrm{J/kgK})$	385	765	686.2	754	4179
$k\,(\mathrm{W/mK})$	400	40	8.9538	1.4013	0.6130
$\sigma\,(\mathrm{s/m})$	59.6×10^6	35×10^6	2.6×10^6	3.5×10^6	5.5×10^{-6}

The system of ODEs can be obtained by substituting Eq. (5) into Eqs. (2)–(4), so that (see Khashi'ie et al. [15], Jamrus et al. [33]):

$$\frac{\mu_{thnf}/\mu_f}{\rho_{thnf}/\rho_f}f''' + 2ff'' - f'^2 - \frac{\sigma_{thnf}/\sigma_f}{\rho_{thnf}/\rho_f}Mf' = 0, \tag{6}$$

$$\frac{1}{\Pr}\frac{k_{thnf}/k_f}{\left(\rho C_p\right)_{thnf}/\left(\rho C_p\right)_f}\theta'' + 2f\theta' - 2f'\theta + \frac{\sigma_{thnf}/\sigma_f}{\left(\rho C_p\right)_{thnf}/\left(\rho C_p\right)_f}EcMf'^2 = 0, \tag{7}$$

$$\begin{aligned} &f(0) = S,\ \ f'(0) = \lambda,\ \ \theta(0) = 1, \\ &f'(\eta) \to 0, \theta(\eta) \to 0 \ \text{ as } \ \eta \to \infty. \end{aligned} \tag{8}$$

In addition to the suction parameter, the study incorporates several key parameters, including M (magnetic field parameter) and Pr (Prandtl number), each of which plays a significant role in governing the flow and thermal characteristics and defined as follows:

$$M = \frac{\sigma_f {M_0}^2}{a\rho_f}, \Pr = \frac{\left(\mu C_p\right)_f}{k_f}, Ec = \frac{u_w^2}{\left(C_p\right)_f (T_w - T_\infty)}. \tag{9}$$

The key physical quantities examined in this study include the skin friction coefficient C_f and the local Nusselt number Nu_r, which are expressed as:

$$C_f = \frac{2\mu_{thnf}\left(\frac{\partial u}{\partial z}\right)_{z=0}}{\rho_f u_w^2}, \quad Nu_r = -\frac{rk_{thnf}\left(\frac{\partial T}{\partial z}\right)_{z=0}}{k_f (T_w - T_\infty)}, \tag{10}$$

Utilizing the similarity transformations from Eq. (5) in Eq. (10), the simplified formulations for the skin friction coefficient and the local Nusselt number are:

$$0.5 {Re_r}^{1/2} C_f = \frac{\mu_{thnf}}{\mu_f} f''(0), \quad {Re_r}^{-1/2} Nu_r = -\frac{k_{thnf}}{k_f}\theta'(0). \tag{11}$$

3 Results and Discussion

The transformed equations are solved numerically using the bvp4c solver in MATLAB, which is a collocation-based finite difference method capable of accurately resolving boundary layer equations with dual solutions. It was chosen for this study due to its high accuracy in solving similarity equations particularly in nanofluid flows and efficiency in handling multiple solutions, making it ideal for studying dual solutions in shrinking flows. The results are generated by numerically solving Eqs. (6)–(8) using the bvp4c solver in the Matlab software. These results are presented in Figs. 1–5, Tables 3 and 4 within a specific range of the parameters as discussed in the previous section. The choice of governing parameters are based on the main references (for comparison between hybrid nanofluid and ternary nanofluid) and also depends on the availability of dual solutions. It is important to discover all the possible solutions since previous literatures have shown that the opposing flow may lead to the occurrence of multiple solutions (see Refs. [36–40]), In this numerical study, the magnitude of physical parameters are $0 \le M \le 0.2$ (magnetic parameter), $0 \le Ec \le 0.2$ (Eckert number), $0 \le \phi_1, \phi_2, \phi_3 \le 0.01$ (volumetric concentration of the Al_2O_3, Cu, and SiO_2/TiO_2, respectively), $S_c \le S \le 1.3$ (suction parameter), and Prandtl number Pr = 6.2 signifies the pure water base fluid. The comparison with the existing model is shown in Table 3. The comparison demonstrates that the present results are aligned with previous finding with 0% error, confirming the accuracy of the bvp4c solver and the validity of the mathematical model. Meanwhile, for future reference and benchmark, Table 4 shows the numerical values for present study considering three types of fluids; alumina-copper/water, alumina-copper-silica/water and alumina-copper-titania/water. The results in Table 4 show that 1% increment of suction enhances the skin friction coefficient and heat transfer efficiency approximately up to 4.17% and 1%, respectively which highlighting its crucial role in stabilizing the opposing flow induced by the

shrinking disk. Additionally, the inclusion of 1% silica nanoparticles concentration to the hybrid nanofluid reduces both skin friction and heat transfer rate by approximately 0.28% and 0.85%, respectively, while 1% titania nanoparticles concentration increases skin friction by 3.02% but results in a slight heat transfer loss of up to 0.61%.

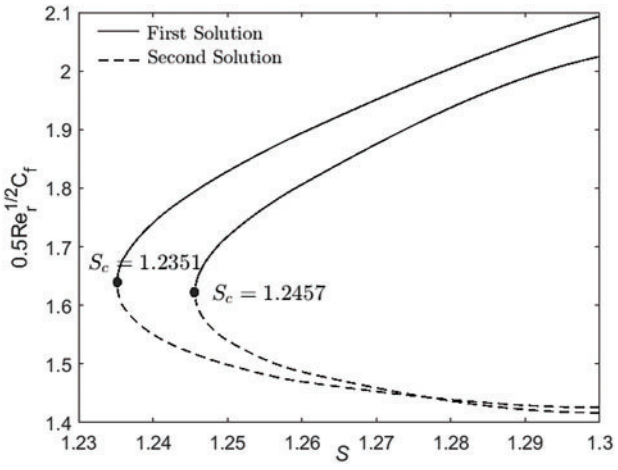

Figure 1: $0.5\mathrm{Re}_r^{1/2}C_f$ towards S for alumina-copper-silica/water $(S_c = 1.2457)$ and alumina-copper-titania/water $(S_c = 1.2351)$ when $\lambda = -1$, $M = Ec = 0.1$ and $\phi_1 = \phi_2 = \phi_3 = 1\%$

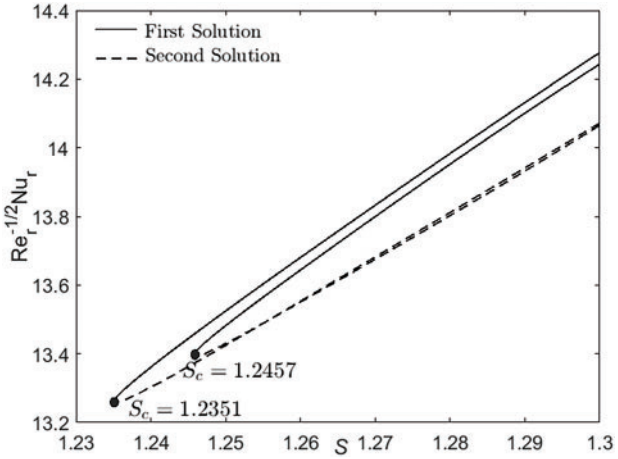

Figure 2: $\mathrm{Re}_r^{-1/2}Nu_r$ towards S for alumina-copper-silica/water $(S_c = 1.2457)$ and alumina-copper-titania/water $(S_c = 1.2351)$ when $\lambda = -1$, $M = Ec = 0.1$ and $\phi_1 = \phi_2 = \phi_3 = 1\%$

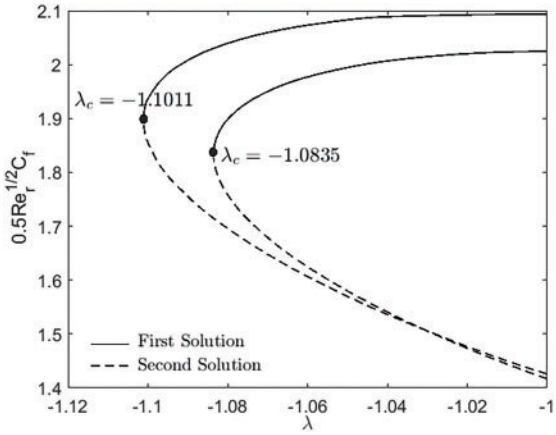

Figure 3: $0.5\mathrm{Re}_r^{1/2}C_f$ towards λ for alumina-copper-silica/water and alumina-copper-titania/water when $M = 0.1$, $S = 1.3$, $\phi_1 = \phi_2 = \phi_3 = 1\%$ and $Ec = 0, 0.1, 0.2$

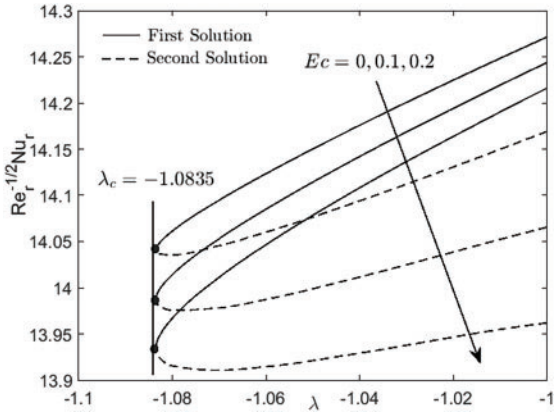

Figure 4: $\mathrm{Re}_r^{-1/2}Nu_r$ towards λ with varied Ec for alumina-copper-silica/water when $M = 0.1$, $S = 1.3$ and $\phi_1 = \phi_2 = \phi_3 = 1\%$

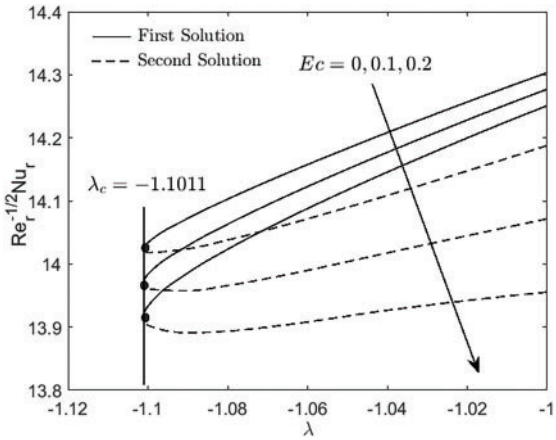

Figure 5: $\mathrm{Re}_r^{-1/2}Nu_r$ towards λ with varied Ec for alumina-copper-titania/water when $M = 0.1$, $S = 1.3$ and $\phi_1 = \phi_2 = \phi_3 = 1\%$

Table 3: Validation of numerical result $f''(0)$ with previous studies when $Ec = S = \phi_3 = \phi_4 = 0$, $\phi_1 = 0.1$, $\phi_2 = 0.05$, $\lambda = 1$ and various M

M	Present	Khashi'ie et al. [15]
0	−1.251214	−1.251214
0.5	−1.440257	−1.440257
1.0	−1.608832	−1.608832
2.0	−1.903452	−1.903452
3.0	−2.159147	−2.159147

Table 4: $0.5\mathrm{Re}_r^{1/2}C_f$ and $\mathrm{Re}_r^{-1/2}Nu_r$ when $\mathbf{Pr = 6.2}, \phi_1 = \phi_2 = 0.01$ and various parameters

Fluid	λ	M	S	Ec	ϕ_3	$0.5\mathrm{Re}_r^{1/2}C_f$		$\mathrm{Re}_r^{-1/2}Nu_r$	
						First	Second	First	Second
Hybrid Nanofluid (alumina-copper/water)	−1	0	1.3	0	0	1.88625	1.48923	14.36868	14.30291
		0.05				1.96637	1.43085	14.38070	14.29190
		0.1				2.03029	1.38906	14.39006	14.28362
			1.31			2.07199	1.38752	14.53422	14.42410
			1.32			2.11200	1.38904	14.67751	14.56470
	−1	0.1	1.3	0.1	0	2.03029	1.38906	14.36442	14.17415
				0.2		2.03029	1.38906	14.33878	14.06468
Alumina-copper-silica/water	−1	0.1	1.3	0.1	0.01	2.02460	1.41665	14.24381	14.06560
					0.02	2.01527	1.44825	14.12184	13.95679
Alumina-copper-titania/water	−1	0.1	1.3	0.1	0.01	2.09345	1.42579	14.27704	14.07163
					0.02	2.15503	1.46336	14.18852	13.96823

Figs. 1 and 2 illustrate the variations in the skin friction coefficient and heat transfer coefficient as a function of the suction parameter. It is evident that the suction parameter plays a critical role in both nanofluid systems and must be incorporated into the physical model to stabilize the opposing flow induced by the shrinking disk. The critical minimum suction values are identified to maintain and stabilize the opposing flow such that $S_c = 1.2457$ for alumina-copper-silica/water and $S_c = 1.2351$ for alumina-copper-titania/water. Moreover, the results reveal that both of the skin friction coefficient and heat transfer rate increase with higher values of the suction parameter. This behaviour can be attributed to the effect of suction in regulating the boundary layer thickness. Suction reduces the thickness of the momentum and thermal boundary layers by drawing fluid closer to the surface, thereby intensifying the velocity and temperature gradients near the wall. These steeper gradients lead to an increase in the skin friction coefficient, which corresponds to greater resistance to flow at the surface, and an enhancement in the heat transfer rate due to more efficient thermal energy exchange at the boundary. Physically, the suction mechanism counteracts the destabilizing effects of the shrinking disk by promoting a more uniform and controlled flow field. This stabilization effect is especially important in flows with opposing tendencies, such as those caused by shrinking surface, which tend to induce reverse flow or recirculation zones without sufficient stabilization. Consequently, the application of an appropriate suction parameter not only maintains flow stability but also augments the interaction between the fluid and the surface, enhancing both frictional forces and heat transfer efficiency.

Fig. 3 compares the skin friction coefficient for two ternary nanofluid combinations which are alumina-copper-silica/water (Al_2O_3-Cu-SiO_2/water) and alumina-copper-titania/water (Al_2O_3-Cu-TiO_2/water) under magnetic field effect with magnitude $M = 0.1$. The results reveal that the critical value of the shrinking disk parameter, which marks the threshold for dual solutions, is higher for the Al_2O_3-Cu-TiO_2/water with $\lambda_c = -1.1011$ as compared to Al_2O_3-Cu-SiO_2/water with $\lambda_c = -1.0835$. The higher λ_c for Al_2O_3-Cu-TiO_2/water implies that this nanofluid can maintain stable flow condition over a broader range of shrinking disk parameter, making it more resistant to flow separation. This difference can be attributed to the enhanced thermophysical properties of the Al_2O_3-Cu-TiO_2 combination. Titanium dioxide (TiO_2) contributes to improved thermal conductivity and stability as compared to silica (SiO_2), resulting in a more robust flow behaviour. This finding underscores the importance of selecting right combination of the nanoparticles that optimize both flow stability and thermal properties for specific engineering applications. In addition, the skin friction coefficient is same when Ec is varied. The reason is the Eckert number generated from the Joule heating only affects the energy equation as well as the thermal performance as demonstrated in Figs. 4 and 5.

Figs. 4 and 5 highlight the critical role of nanoparticle composition in determining the thermal performance of nanofluids under the influence of Eckert number. Both nanofluids exhibit a decrease in $\mathrm{Re}_r^{-1/2} Nu_r$ (heat transfer rate) with the increasing values of Ec. However, the alumina-copper-titania/water nanofluid demonstrates a superior ability to sustain heat transfer rate due to its enhanced thermal conductivity. This suggests that applications requiring high heat transfer efficiency under dissipative conditions should prioritize nanofluids with titanium-based nanoparticles. Physically, the Eckert number signifies the influence of viscous dissipation in the energy equation, quantifying the conversion of kinetic energy into internal energy (heat form) within the fluid. When $Ec = 0$, viscous dissipation is entirely absent, meaning there is no additional heat generated due to the fluid motion which consequently, enhances the local Nusselt number. The thermal boundary layer becomes more efficient at transferring heat when no energy is dissipated into the fluid as heat. Another physical judgment is under shrinking flow ($\lambda < 0$), the adverse pressure gradient induced by the surface's motion compresses the boundary layer. This compression increases the velocity and temperature gradients near the surface, thereby amplifying the heat transfer rate. When $Ec = 0$, the absence of viscous dissipation ensures that this enhanced gradient is not counteracted by additional heat generated within the fluid, leading to a significantly higher heat transfer rate.

4 Conclusions

This study explored the heat transfer and flow dynamics of a ternary hybrid nanofluid (THNF) consisting of alumina, copper, and silica/titania nanoparticles over a permeable shrinking disk, incorporating the effects of suction, magnetic field, and Joule heating. The findings highlight the critical role of suction in stabilizing opposing flow, with an increase of 1% suction enhancing the skin friction coefficient by 4.17% and heat transfer efficiency by approximately 1%. The comparative analysis between alumina-copper-silica and alumina-copper-titania nanofluids revealed that:

- Al_2O_3-Cu-TiO_2/water exhibits superior thermal performance, attributed to its higher thermal conductivity.

- Al_2O_3-Cu-SiO_2 water shows a slight reduction in both skin friction and heat transfer, confirming the influence of nanoparticle composition on thermal efficiency.

- The study identified critical suction values necessary for flow stabilization, providing insights into controlling boundary layer separation in shrinking flows.

These findings establish Al_2O_3-Cu-TiO_2/water as a promising solution for high-performance cooling systems, energy-efficient heat exchangers, and industrial thermal management applications. Future research should explore unsteady flow behavior, non-Newtonian ternary nanofluids, and machine-learning-based optimization techniques to further refine THNF thermal performance.

Acknowledgement: The authors would like to thank Universiti Teknikal Malaysia Melaka, Universiti Putra Malaysia and Babeş-Bolyai University for the research support.

Funding Statement: This research was funded by Universiti Teknikal Malaysia Melaka, through Fakulti Teknologi dan Kejuruteraan Mekanikal (FTKM)'s publication fund-K23003.

Author Contributions: The authors confirm contribution to the paper as follows: study conception and mathematical formulation: Umi Nadrah Hussein, Najiyah Safwa Khashi'ie, Norihan Md Arifin, Ioan Pop; data collection: Umi Nadrah Hussein, Najiyah Safwa Khashi'ie; analysis and interpretation of results: Umi Nadrah Hussein, Najiyah Safwa Khashi'ie; draft manuscript preparation: Umi Nadrah Hussein, Najiyah Safwa Khashi'ie, Norihan Md Arifin. All authors reviewed the results and approved the final version of sthe manuscript.

Availability of Data and Materials: Not applicable.

Ethics Approval: Not applicable.

Conflicts of Interest: The authors declare no conflicts of interest to report regarding the present study.

References

1. Habibishandiz M, Saghir MZ. A critical review of heat transfer enhancement methods in the presence of porous media, nanofluids, and microorganisms. Therm Sci Eng Prog. 2022;30(10):101267. doi:10.1016/j.tsep.2022.101267.
2. Younes H, Mao M, Murshed SS, Lou D, Hong H, Peterson GP. Nanofluids: key parameters to enhance thermal conductivity and its applications. Appl Therm Eng. 2022;207:118202. doi:10.1016/j.applthermaleng.2022.118202.
3. Okonkwo EC, Wole-Osho I, Almanassra IW, Abdullatif YM, Al-Ansari T. An updated review of nanofluids in various heat transfer devices. J Therm Anal Calorim. 2021;145(6):2817–72. doi:10.1007/s10973-020-09760-2.
4. Nabil MF, Azmi WH, Hamid KA, Zawawi NN, Priyandoko G, Mamat R. Thermo-physical properties of hybrid nanofluids and hybrid nanolubricants: a comprehensive review on performance. Int Comm Heat Mass Transf. 2017;83(6):30–9. doi:10.1016/j.icheatmasstransfer.2017.03.008.
5. Adun H, Kavaz D, Dagbasi M. Review of ternary hybrid nanofluid: synthesis, stability, thermophysical properties, heat transfer applications, and environmental effects. J Cleaner Prod. 2021;328:129525. doi:10.1016/j.jclepro.2021.129525.
6. Oladapo OA, Ajala OA, Akindele AO, Aselebe LO, Obalalu AM, Ohaegbue AD, et al. Analysis of variable properties on ternary and tetra hybrid nanofluids using Blasius Rayleigh-Stokes time dependent variable: a model for solar aeronautical engineering. Int J Thermofluids. 2024;23:100775.
7. Yu Y, Du J, Hou J, Jin X, Wang R. Investigation into the underlying mechanisms of the improvement of thermal conductivity of the hybrid nanofluids. Int J Heat Mass Transf. 2024;226:125468.
8. Takabi B, Salehi S. Augmentation of the heat transfer performance of a sinusoidal corrugated enclosure by employing hybrid nanofluid. Adv Mech Eng. 2014;6:147059.
9. Devi SA, Devi SS. Numerical investigation of hydromagnetic hybrid Cu-Al_2O_3/water nanofluid flow over a permeable stretching sheet with suction. Int J Nonlin Sci Numer Simul. 2016;17(5):249–57.
10. Devi SS, Devi SA. Numerical investigation of three-dimensional hybrid Cu-Al_2O_3/water nanofluid flow over a stretching sheet with effecting Lorentz force subject to Newtonian heating. Canadian J Phys. 2016;94(5):490–6.
11. Devi SS, Devi SA. Heat transfer enhancement of Cu-Al_2O_3/water hybrid nanofluid flow over a stretching sheet. J Niger Math Soc. 2017;36(2):419–33.

12. Waqas H, Farooq U, Naseem R, Hussain S, Alghamdi M. Impact of MHD radiative flow of hybrid nanofluid over a rotating disk. Case Stud Therm Eng. 2021;26:101015.
13. Khan U, Zaib A, Abu Bakar S, Ishak A. Unsteady stagnation-point flow of a hybrid nanofluid over a spinning disk: analysis of dual solutions. Neural Comp Appl. 2022;34(10):8193–210.
14. Bilal M, Saeed A. Numerical computation for the dual solution of Sisko hybrid nanofluid flow through a heated shrinking/stretching porous disk. Int J Ambient Energy. 2022;43(1):8802–11.
15. Khashi'ie NS, Arifin NM, Nazar R, Hafidzuddin EH, Wahi N, Pop I. Magnetohydrodynamics (MHD) axisymmetric flow and heat transfer of a hybrid nanofluid past a radially permeable stretching/shrinking sheet with Joule heating. Chin J Phys. 2020;64:251–63.
16. Khashi'ie NS, Arifin NM, Pop I. Unsteady axisymmetric flow and heat transfer of a hybrid nanofluid over a permeable stretching/shrinking disc. Int J Numer Methods Heat Fluid Flow. 2021;31(6):2005–21. doi:10.1108/HFF-07-2020-0421.
17. Li YX, Muhammad T, Bilal M, Khan MA, Ahmadian A, Pansera BA. Fractional simulation for Darcy-Forchheimer hybrid nanoliquid flow with partial slip over a spinning disk. Alex Eng J. 2021;60(5):4787–96. doi:10.1016/j.aej.2021.03.062.
18. Ali B, Mishra NK, Rafique K, Jubair S, Mahmood Z, Eldin SM. Mixed convective flow of hybrid nanofluid over a heated stretching disk with zero-mass flux using the modified Buongiorno model. Alex Eng J. 2023;72(12):83–96. doi:10.1016/j.aej.2023.03.078.
19. Tassaddiq A, Khan S, Bilal M, Gul T, Mukhtar S, Shah Z, et al. Heat and mass transfer together with hybrid nanofluid flow over a rotating disk. AIP Adv. 2020;10(5):055317. doi:10.1063/5.0010181.
20. Rahman NA, Khashi'ie NS, Hamzah KB, Zainal NA, Waini I, Pop I. Axisymmetric hybrid nanofluid flow over a radially shrinking disk with heat generation and magnetic field effects. JP J Heat Mass Transf. 2024;37(3):365–75. doi:10.17654/0973576324025.
21. Jamrus FN, Waini I, Khan U, Ishak A. Effects of magnetohydrodynamics and velocity slip on mixed convective flow of thermally stratified ternary hybrid nanofluid over a stretching/shrinking sheet. Case Stud Therm Eng. 2024;55(66):104161. doi:10.1016/j.csite.2024.104161.
22. Jamrus FN, Ishak A, Waini I, Khan U, Siddiqui MI, Madhukesh JK. Aspects of non-unique solutions for hiemenz flow filled with ternary hybrid nanofluid over a stretching/shrinking sheet. Adv Math Phys. 2024;2024(1):7253630. doi:10.1155/2024/7253630.
23. Hussein UN, Khashi'ie NS, Arifin NM, Pop I. Magnetohydrodynamics (MHD) flow of ternary nanofluid and heat transfer past a permeable cylinder with velocity slip. Chin J Phys. 2025;93(15):328–39. doi:10.1016/j.cjph.2024.12.002.
24. Hussein UN, Khashi'ie NS, Hamzah KB, Arifin NM, Pop I. Joule heating effect on ternary nanofluid flow and heat transfer over a permeable cylinder. JP J Heat Mass Transf. 2024;37(6):831–41. doi:10.17654/0973576324051.
25. Mahmood Z, Khan U, Saleem S, Rafique K, Eldin SM. Numerical analysis of ternary hybrid nanofluid flow over a stagnation region of stretching/shrinking curved surface with suction and Lorentz force. J Magn Mag Mater. 2023;573(3):170654. doi:10.1016/j.jmmm.2023.170654.
26. Mahmood Z, Ahammad NA, Alhazmi SE, Khan U, Bani-Fwaz MZ. Ternary hybrid nanofluid near a stretching/shrinking sheet with heat generation/absorption and velocity slip on unsteady stagnation point flow. Int J Mod Phys B. 2022;36(29):2250209. doi:10.1142/S0217979222502095.
27. Mumtaz M, Islam S, Ullah H, Dawar A, Shah Z. A numerical approach to radiative ternary nanofluid flow on curved geometry with porous media and multiple slip constraints. ZAMM-J Appl Math Mech/Z Für Angew Math Und Mech. 2024;104(10):e202300914. doi:10.1002/zamm.202300914.
28. Mumtaz M, Islam S, Ullah H, Dawar A, Shah Z. A numerical approach to radiative ternary nanofluid flow on curved geometry with cross-diffusion and second order velocity slip constraints. Int J Heat Fluid Flow. 2024;105:109255. doi:10.1016/j.ijheatfluidflow.2023.109255.
29. Shinwari W, Hayat T, Abbas Z, Momani S. A numerical study on the flow of water-based ternary hybrid nanomaterials on a stretchable curved sheet. Nanoscale Adv. 2023;5(22):6249–61. doi:10.1039/D3NA00572K.

30. Alharbi AA. Thermal analysis of heat transport in a slip flow of ternary hybrid nanofluid with suction upon a stretching/shrinking sheet. Case Stud Therm Eng. 2024;54(25–26):103965. doi:10.1016/j.csite.2023.103965.
31. Khan M, Alhowaity A, Imran M, Hussien M, Alroobaea R, Anwar MS. Advanced numerical simulation techniques in MHD fluid flow analysis using distributed fractional order derivatives and Cattaneo heat flux model. ZAMM-J Appl Math Mech/Z Für Angew Math Und Mech. 2024;104(5):e202300622. doi:10.1002/zamm.202300622.
32. Khan M, Imran M. ANN-driven insights into heat and mass transfer dynamics in chemical reactive fluids across variable-thickness surfaces. Heat Transf. 2024;53(8):4551–71. doi:10.1002/htj.23144.
33. Jamrus FN, Ishak A, Waini I, Khan U. Radiative influence on axisymmetric ternary hybrid nanofluid flow with convective boundary conditions over a nonlinearly permeable stretching/shrinking disk. Int J Numer Methods Heat Fluid Flow. 2024;34(12):4333–61. doi:10.1108/HFF-04-2024-0324.
34. Memon MA, Jacob K, Lanjwani HB, Mahmoud EE. Darcy-Forchheimer MHD micropolar water based hybrid nanofluid flow, heat and mass transfer features past on stretching/shrinking surface with slip and radiation effects. Results Eng. 2024;23(1):102534. doi:10.1016/j.rineng.2024.102534.
35. Buongiorno J. Convective transport in nanofluids. J Heat Transf. 2006;128(3):240–50. doi:10.1115/1.2150834.
36. Sarfraz M, Yasir M, Khan M. Multiple solutions for non-linear radiative mixed convective hybrid nanofluid flow over an exponentially shrinking surface. Sci Rep. 2023;13(1):3443. doi:10.1038/s41598-023-29892-3.
37. Lund LA, Omar Z, Khan I, Seikh AH, Sherif ES, Nisar KS. Stability analysis and multiple solution of Cu-Al_2O_3/H_2O nanofluid contains hybrid nanomaterials over a shrinking surface in the presence of viscous dissipation. J Mater Res Tech. 2020;9(1):421–32. doi:10.1016/j.jmrt.2019.10.071.
38. Ahmed S, Chen ZM, Ishaq M. Multiple solutions in magnetohydrodynamic stagnation flow of hybrid nanofluid past a sheet with mathematical chemical reactions model and stability analysis. Phys Fluids. 2023;35(7):072002. doi:10.1063/5.0157429.
39. Yan L, Dero S, Khan I, Mari IA, Baleanu D, Nisar KS, et al. Dual solutions and stability analysis of magnetized hybrid nanofluid with Joule heating and multiple slip conditions. Processes. 2020;8(3):332. doi:10.3390/pr8030332.
40. Khan M, Qamar M, Alqahtani AS, Malik MY. On multiple solutions of cubic catalysis chemically reactive flow of hybrid nanofluids. Results Eng. 2024;24(6):103404. doi:10.1016/j.rineng.2024.103404.